



## Multi-User Phase Noises on Uplink MIMO-OFDM Systems

Xiaoming Chen<sup>\*</sup><sup>(1)</sup>, Andreas Wolfgang<sup>(2)</sup>, and Tommy Svensson<sup>(3)</sup>

(1) School of Electronic and Information Engineering, Xi'an Jiaotong University, Xi'an 710049, China

(2) Qamcom Research & Technology AB, Gothenburg 41285, Sweden

(3) Department of Electrical Engineering, Chalmers University of Technology, Gothenburg 41296, Sweden

### Abstract

In this paper, the effect of phase noises (PNs) of multiple users on orthogonal frequency division multiplexing (OFDM) based multiple-input multiple-output (MIMO) systems is studied. It is assumed that each of the users has a single antenna, whereas the base station (BS) has multiple antennas and use zero-forcing (ZF) decoder for multi-user detection. Since each user is equipped with an independent oscillator, the received uplink (UL) signal at each BS antenna is corrupted by all of these independent PNs. Analytical study on the performances of the MIMO-OFDM system in the presence of multiple PNs is presented and the analytical results are verified by simulations.

### 1. Introduction

The orthogonal frequency division multiplexing (OFDM) technique can effectively turn the frequency-selective channel into multiple frequency-flat channels at different subcarriers, allowing simple one-tap channel equalization. And it can be readily combined with multiple-input multiple-output (MIMO) techniques to exploit spatial multiplexing and/or diversity gain. As a result, MIMO-OFDM systems are used ubiquitously in modern telecommunications. Unfortunately, MIMO-OFDM systems are sensitive to oscillator phase noises [1-12], which cause common phase error (CPE) and intercarrier interference (ICI). The PN effect on single-user MIMO-OFDM (SU-MIMO-OFDM) systems has been well studied in the literature [1-8]. Assuming the base station (BS) antennas share a common oscillator, the downlink (DL) of the multi-user MIMO-OFDM (MU-MIMO-OFDM) system (at each user) is similar to the single-user case. In the uplink (UL) transmission, however, the received signal at the BS is corrupted by multiple PNs. Since the PNs from different users are independent, the PN estimation in the UL is more complex than that in the DL. For this reason, we focus on the multi-user PN effect in the UL case in this work.

There are a few works studying the PN effect on UL MU-MIMO-OFDM systems [9-12]. While [9] considered multiple PNs from the users together with another PN at

the BS, [10] and [11] only considered multiple PNs at the BS (with large antenna array) by assuming PN-free users. The PNs from the users are mixed at each BS antenna, whereas the PNs (of multiple oscillators) at the BS are uncoupled. Therefore, PN estimation in the former is more challenging than that in the latter. For example, the CPEs of multi-user PNs must be jointly estimated [9], whereas the simple CPE correction method [2] (for SU-MIMO-OFDM) can be applied to track each of the BS PNs individually [10]. Therefore, we focus on the effect of multi-user PNs in this work.

It is difficult to compensate the ICI effects of multiple transmit PNs at the receiver [6]. A PN compensation scheme that mitigates the multiple transmit PNs and a receive PN separately was proposed in [12] for multi-node backhauling. Nevertheless, the scheme requires feedback loops with direct RF sampling and, therefore, is not feasible for the considered multi-user scenario in this work. Unlike [9] and [12] that have only numerical simulations, we analytically derive the error vector magnitude (EVM) [5, 6], performance of MU-MIMO-OFDM, assuming the CPEs of different PNs can be perfectly estimated. The analytical results give more insight into the ICI effect of multi-user PNs. Finally, the ICI effect of multi-user PNs for different numbers of BS antennas and users are studied analytically and experimentally (by simulations). Good agreement between simulation and theory is observed.

*Notations:* Throughout this paper,  ${}^*$ ,  ${}^T$ ,  ${}^H$ , and  ${}^\dagger$  denote complex conjugate, transpose, Hermitian, and Moore-Penrose pseudoinverse, respectively. Lowercase bold letter ( $\mathbf{x}$ ) and uppercase bold letter ( $\mathbf{X}$ ) represent column vector and matrix, respectively.  $\mathbf{I}_M$  is the  $M \times M$  identity matrix.  $\text{diag}(\mathbf{x})$  denotes the diagonal matrix whose diagonal elements are given by  $\mathbf{x}$ .  $\|\mathbf{x}\|_2$  is the Euclidean norm of  $\mathbf{x}$ .  $\text{Tr}(\mathbf{X})$  represents the trace of  $\mathbf{X}$ .  $\otimes$  denotes the Kronecker product.  $E$  represents mathematical expectation.

### 2. System Model

For simplicity, we assume  $K$  users (each equipped with a single antenna along with a free-running oscillator) and  $M$

( $> K$ ) antennas at the BS. The BS uses zero-forcing (ZF) decoder for multi-user detection. In order to focus on the PN effect, we assume perfect channel estimation and that the cyclic prefix (CP) of the OFDM symbol is longer than the channel length.

Let  $N$  be the number of OFDM subcarriers,  $\mathbf{F}$  be an  $N \times N$  discrete Fourier transform (DFT) matrix, whose elements are given by  $\exp(-j2\pi kl/N)/\sqrt{N}$  ( $k, l = 0, \dots, N-1$ ), and  $\boldsymbol{\varphi}_i$  and  $\boldsymbol{\theta}$  be  $N \times 1$  vectors consisting the time-domain PNs during one OFDM symbol at the  $i$ th user ( $i = 1, \dots, K$ ) and at the BS, respectively. The frequency-domain expression of the UL transmission (from  $K$  users to the BS) in the presence of PNs is given as

$$\mathbf{y} = (\mathbf{G}_R \otimes \mathbf{I}_M) \mathbf{H} \mathbf{G}_T \mathbf{x} + \mathbf{w} \quad (1)$$

where  $\mathbf{H}$  is a  $MN \times KN$  block diagonal channel matrix whose  $k$ th diagonal block entry  $\mathbf{H}_k$  is the  $M \times K$  channel transfer functions (CTFs) at the  $k$ th subcarrier,  $\mathbf{x} = [\mathbf{x}_0^T \ \mathbf{x}_1^T \ \dots \ \mathbf{x}_{N-1}^T]^T$  is the  $KN \times 1$  signal vector with  $\mathbf{x}_k$  denoting the  $K \times 1$  transmitted signal vector (from all the users) at the  $k$ th subcarrier,  $\mathbf{y} = [\mathbf{y}_0^T \ \mathbf{y}_1^T \ \dots \ \mathbf{y}_{N-1}^T]^T$  is the  $MN \times 1$  signal vector with  $\mathbf{y}_k$  denoting the  $M \times 1$  received signal vector at the  $k$ th subcarrier,  $\mathbf{w}$  is a  $MN \times 1$  additive white Gaussian noise (AWGN) vector,  $\mathbf{G}_R = \mathbf{F} \text{diag}(\exp(j\boldsymbol{\theta})) \mathbf{F}^H$  is an  $N \times N$  matrix of the PN spectral components of the BS oscillator, and  $\mathbf{G}_T$  is a  $KN \times KN$  matrix consisting the  $N$  spectral components of the PNs of all the  $K$  users. The  $(k, l)$ th entry of  $\mathbf{G}_R$  is denoted as  $g_{(k-l)_N}^{\text{Rx}}$ , where  $(k-l)_N$  denotes  $(k-l) \bmod N$ . The  $(k, l)$ th block of  $\mathbf{G}_T$  is  $\text{diag}(\mathbf{g}_{(k-l)_N}^{\text{Tx}})$ , where the  $K \times 1$  vector  $\mathbf{g}_{(k-l)_N}^{\text{Tx}}$  consists of the corresponding spectral components of the PNs from the  $K$  users. By separating the CPE and ICI terms  $\mathbf{G}_T = \mathbf{I}_N \otimes \text{diag}(\mathbf{g}_0^{\text{Tx}}) + \mathbf{P}_T$  and  $\mathbf{G}_R = g_0^{\text{Rx}} \mathbf{I}_N + \mathbf{P}_R$ , (1) can be rewritten as

$$\mathbf{y} = g_0^{\text{Rx}} \mathbf{H} (\mathbf{I}_N \otimes \text{diag}(\mathbf{g}_0^{\text{Tx}})) \mathbf{x} + \mathbf{e} + \mathbf{w} \quad (2)$$

where  $g_0^{\text{Rx}}$  is the CPE of the PN at the BS,  $\mathbf{g}_0^{\text{Tx}}$  consists of the CPEs of the PNs from the  $K$  users, and the ICI term  $\mathbf{e}$  is

$$\mathbf{e} = (\mathbf{P}_R \otimes \mathbf{I}_M) \mathbf{H} \mathbf{P}_T \mathbf{x} + g_0^{\text{Rx}} \mathbf{H} \mathbf{P}_T \mathbf{x} + (\mathbf{P}_R \otimes \mathbf{I}_M) \mathbf{H} (\mathbf{I}_N \otimes \text{diag}(\mathbf{g}_0^{\text{Tx}})) \mathbf{x} \quad (3).$$

### 3. Performance Analysis

The receive signal at the  $k$ th subcarrier is

$$\mathbf{y}_k = \mathbf{H}_k \text{diag}(\mathbf{g}_0) \mathbf{x}_k + \mathbf{e}_k + \mathbf{w}_k \quad (4)$$

where  $\mathbf{g}_0 = g_0^{\text{Rx}} \mathbf{g}_0^{\text{Tx}}$ , and  $\mathbf{e}_k$  and  $\mathbf{w}_k$  denote ICIs and AWGNs at the  $k$ th subcarrier, respectively. The CPEs  $\mathbf{g}_0$  can be estimated as [9]

$$\hat{\mathbf{g}}_0 = \frac{1}{N_p} \sum_{k \in S_p} (\mathbf{H}_k \text{diag}(\mathbf{x}_k))^{\dagger} \mathbf{y}_k \quad (5)$$

where  $S_p$  denotes the set of the  $N_p$  scattered pilots. The CPEs can be corrected at the ZF decoder as

$$\hat{\mathbf{x}}_k = \text{diag}(\hat{\mathbf{g}}_0)^{-1} \mathbf{H}_k^{\dagger} \mathbf{y}_k \quad (6)$$

where  $\hat{\mathbf{x}}_k$  denote the detected signals at the  $k$ th subcarrier.

In order to focus on the ICI effects of multi-user PNs, we assume perfect channel estimation and perfect estimation of CPEs. For simplicity, we ignore the BS PN and focus on multi-user PNs; and assume independent multi-tap Rayleigh fading channel. For notational convenience, we drop the superscript  $^{\text{Tx}}$  hereafter.

The signal at the  $k$ th subcarrier after ZF decoder is

$$\mathbf{r}_k = \text{diag}(\mathbf{g}_0) \mathbf{x}_k + \sum_{l=0, l \neq k}^{N-1} \text{diag}(\mathbf{g}_{(k-l)_N}) \mathbf{x}_l + \mathbf{H}_k^{\dagger} \mathbf{w}_k \quad (7).$$

The EVM at the  $k$ th subcarrier is

$$\xi_k = \frac{\mathbb{E} \left[ \left\| \sum_{l \neq k} \text{diag}(\mathbf{g}_{(k-l)_N}) \mathbf{x}_l \right\|_2^2 \right] + \mathbb{E} \left[ \left\| \mathbf{H}_k^{\dagger} \mathbf{w}_k \right\|_2^2 \right]}{\mathbb{E} \left[ \left\| \text{diag}(\mathbf{g}_0) \mathbf{x}_k \right\|_2^2 \right]} \quad (8).$$

Assuming the subcarrier symbols are independent and identically distributed with a variance of  $\sigma_x^2$ , i.e.,  $\mathbb{E}[\mathbf{x}_k \mathbf{x}_k^H] = \sigma_x^2 \mathbf{I}_K$ , the power contributions of the useful signal (with known CPEs) and ICI term can be expressed as

$$\begin{aligned} \mathbb{E} \left[ \left\| \text{diag}(\mathbf{g}_0) \mathbf{x}_k \right\|_2^2 \right] &= \sigma_x^2 \mathbb{E} \left[ \left\| \mathbf{g}_0 \right\|_2^2 \right], \\ \mathbb{E} \left[ \left\| \sum_{l \neq k} \text{diag}(\mathbf{g}_{(k-l)_N}) \mathbf{x}_l \right\|_2^2 \right] &= \sigma_x^2 \mathbb{E} \left[ \sum_{l \neq k} \left\| \mathbf{g}_{(k-l)_N} \right\|_2^2 \right] \end{aligned} \quad (9)$$

respectively.

The PN of a free-running oscillator can be modeled by the Wiener process, whose discrete-time expression is

$$\phi(n+1) = \phi(n) + \eta(n) \quad (10)$$

where  $\phi$  is the phase noise and  $\eta$  is a zero-mean Gaussian random variable whose variance is  $4\pi\beta T_s$  with  $T_s$  denoting

the sampling duration and  $\beta$  representing the 3-dB bandwidth of the PN. Assuming the oscillators at different users are of the same quality (i.e., PNs from different user have the same 3-dB bandwidth  $\beta$ ),

$$\begin{aligned} \mathbb{E}\left[\|\mathbf{g}_0\|_2^2\right] &= K\mathbb{E}\left[|g_0|^2\right] = K\sigma_{\text{CPE}}^2 \\ \mathbb{E}\left[\sum_{l \neq k} \|\mathbf{g}_{(k-l)N}\|_2^2\right] &= K\mathbb{E}\left[\sum_{l \neq k} |g_{(k-l)N}|^2\right] = K\sigma_{\text{ICI}}^2 \end{aligned} \quad (11).$$

Note that  $\mathbb{E}\left[\sum_{l \neq k} |g_{(k-l)N}|^2\right] = \mathbb{E}\left[\sum_{k \neq 0} |g_k|^2\right]$ . Let

$$g_{(k-l)N} \Big|_{l=0} = g_k = \frac{1}{N} \sum_n \exp(j\phi(n)) \exp(-j2\pi kn/N) \quad (12),$$

the total power of the PN is given as

$$\begin{aligned} \sum_{k=0}^{N-1} |g_k|^2 &= \frac{1}{N^2} \sum_{k=0}^{N-1} \left[ \sum_n \sum_m \exp(j(\phi(n)-\phi(m))) \exp\left(j\frac{2\pi k(m-n)}{N}\right) \right] \\ &= \frac{1}{N^2} \sum_n \sum_m \exp(j(\phi(n)-\phi(m))) \sum_{k=0}^{N-1} \exp\left(j\frac{2\pi k(m-n)}{N}\right) \end{aligned} \quad (13)$$

$$\text{where } \sum_{k=0}^{N-1} \exp\left(j\frac{2\pi k(m-n)}{N}\right) = \begin{cases} N, & m=n \\ 0, & m \neq n \end{cases}.$$

Hence,

$$\sigma_{\text{CPE}}^2 + \sigma_{\text{ICI}}^2 = \mathbb{E}\left[\sum_{k=0}^{N-1} |g_k|^2\right] = \frac{1}{N^2} N \times N = 1 \quad (14).$$

Using the DFT expression (12),  $\sigma_{\text{CPE}}^2$  can be derived as

$$\begin{aligned} \mathbb{E}\left[|g_0|^2\right] &= \mathbb{E}\left[\sum_n \sum_m \exp(j(\phi(n)-\phi(m)))\right] \\ &= \frac{1}{N^2} \sum_n \sum_m \exp(-2\pi\beta|n-m|T_s) \end{aligned} \quad (15)$$

where the last step is derived using the characteristic function. Once  $\sigma_{\text{CPE}}^2$  is known,  $\sigma_{\text{ICI}}^2$  can be readily derived as

$$\mathbb{E}\left[\sum_{k \neq 0} |g_k|^2\right] = 1 - \frac{1}{N^2} \sum_n \sum_m \exp(-2\pi\beta|n-m|T_s) \quad (16).$$

Since  $\mathbf{H}_k^\dagger = (\mathbf{H}_k^H \mathbf{H}_k)^{-1} \mathbf{H}_k^H$  and  $\mathbb{E}\left[\mathbf{w}_k \mathbf{w}_k^H\right] = \sigma_w^2 \mathbf{I}_M$ , the noise power (after the ZF decoder) is given as

$$\mathbb{E}\left[\|\mathbf{H}_k^\dagger \mathbf{w}_k\|_2^2\right] = \sigma_w^2 \text{Tr}\left\{\mathbb{E}\left[(\mathbf{H}_k^H \mathbf{H}_k)^{-1}\right]\right\} \quad (17).$$

For spatially white Rayleigh fading multipath channel  $\mathbf{H}_k$  and  $M > K$ ,  $(\mathbf{H}_k^H \mathbf{H}_k)^{-1}$  follows inverse (central) Wishart distribution, whose mean is  $\mathbf{I}_K/(M-K)$  [13]. Hence (17) boils down to

$$\mathbb{E}\left[\|\mathbf{H}_k^\dagger \mathbf{w}_k\|_2^2\right] = \frac{\sigma_w^2 K}{M-K} \quad (18).$$

Denoting the signal-to-noise ratio (SNR) as  $\gamma_0 = \sigma_x^2 / \sigma_w^2$ , and combining (8), (9), (11), (15), (16), and (18), the EVM at the  $k$ th subcarrier can be derived as

$$\xi_k = \frac{(M-K)\gamma_0 \left( N^2 - \sum_{n=0}^{N-1} \sum_{m=0}^{N-1} \exp(-2\pi\beta|n-m|T_s) \right) + N^2}{(M-K)\gamma_0 \sum_{n=0}^{N-1} \sum_{m=0}^{N-1} \exp(-2\pi\beta|n-m|T_s)} \quad (19).$$

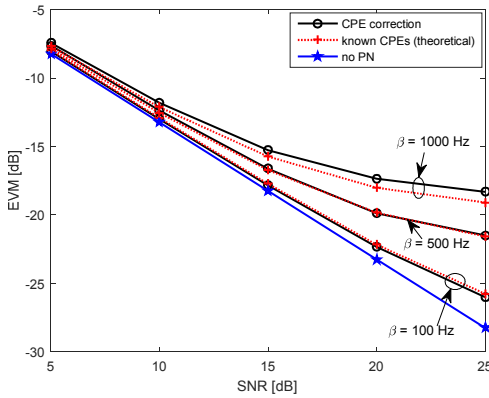
As can be seen,  $\xi_k$  is independent of the subcarrier index  $k$ , hence, the EVM averaged over all the subcarriers is also given by (19). It can be concluded from (19) that the EVM performance degrades with increasing  $\beta$  (the 3-dB bandwidth of the PN) and/or with increasing user number  $K$  (for a given number of BS antennas  $M$ ), and improves with increasing  $M$  (for a given  $K$ ).

## 4. Simulations

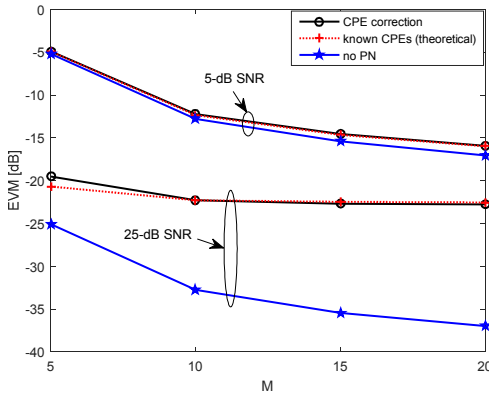
Throughout the section, we make the following assumptions. There are 512 subcarriers including 32 scattered pilots. The remaining active subcarrier are loaded with QAM symbols. The multipath fading channel is a 4-tap Rayleigh fading channel, where the taps are at the 0, 20, 30, and 60th time samples with equal average tap gain of 0.25. (Note that the analysis is valid for any power delay profile [14, 15].) The channel stay constant within 40 OFDM symbols after which an independent channel realization is drawn (in total 100 channel realizations are generated). The CP length of the OFDM is set to 64 so that there is no inter-symbol interference due to the delay spread. The PNs from different users are independent yet follow the same (Wiener process) distribution with the same 3-dB PN bandwidth  $\beta$ .

Figure 1 shows the EVM performance of the MU-MIMO-OFDM system (in the presence of multiple PNs) with two users and four BS antennas. As a reference, the ideal case (no PN) is also plotted in the same figure. As can be seen, with modest PN ( $\beta \leq 500$  Hz) the simulated EVM with CPE correction agrees well with that of the theoretical one (19). This implies that the CPE correction presented in Section IV can eliminate the CPEs of the multiple PNs. Note that, as  $\beta$  increases, the CPE estimation (5) becomes less accurate. As a result, it is also shown that the EVM performance with CPE correction is slightly worse than its theoretical counterpart as  $\beta$  increases up to 1000 Hz.

Figure 2 shows the EVM performance of the PN corrupted MU-MIMO-OFDM system (with four users) as a function of BS antenna number (under different SNRs). The 3-dB PN bandwidth is set to 500 Hz. As references, the EVM of the corresponding ideal cases (no PN) are also plotted in the same figure. As can be seen, the EVM performance improves as the number of BS antennas increases at low (5-dB) SNR. At high (25-dB) SNR, however, the EVM performance improvement becomes insignificant beyond ten BS antennas.



**Figure 1.** EVM performance of MU-MIMO-OFDM ( $K=2$ ,  $M=4$ ) with different 3-dB PN bandwidths.



**Figure 2.** EVM performance of MU-MIMO-OFDM ( $K=4$ ,  $\beta=500$  Hz) as a function of BS antenna number ( $M$ ) under different SNRs.

## 6. Acknowledgements

The research leading to these results received funding from the European Commission H2020 programme under grant agreement no. 671650 (5G PPP mmMAGIC project).

## 7. References

1. T. C. W. Schenk, X.-J. Tao, P. F. M. Smulders, et al., "On the influence of phase noise induced ici in MIMO OFDM systems," *IEEE Commun. Lett.*, **9**, 8, Aug. 2005, pp. 682-684.
2. P. Liu, S. Wu, and Y. Bar-Ness, "A Phase noise mitigation scheme for MIMO WLANs with spatially correlated and imperfectly estimated channels," *IEEE Commun. Lett.*, **10**, 3, pp. 141-143, Mar. 2006.
3. S. Bittner, E. Zimmermann, and G. Fettweis, "Exploiting phase noise properties in the design of MIMO-OFDM receivers," in *Proc. IEEE Wireless Networking Conf. (WCNC)*, Mar. 2008.
4. R. Corvaja and A. G. Armada, "SINR degradation in MIMO-OFDM systems with channel estimation errors and partial phase noise compensation," *IEEE Trans. Commun.*, **58**, 8, pp. 2199-2203, Aug., 2010.
5. R. Hamila, Ö. Özdemir, and N. Al-Dahir, "Beamforming OFDM performance under joint phase noise and I/Q imbalance," *IEEE Trans. Veh. Technol.*, **65**, 5, pp. 2978-2989, May 2016.
6. X. Chen, H. Wang, W. Fan, Y. Zou, A. Wolfgang, T. Svensson, and J. Luo, "Phase noise effect on MIMO-OFDM systems with common and independent oscillators," *Wireless Communications and Mobile Computing*, **2017**, pp. 1-12, 2017.
7. R. Krishnan, M. R. Khanzadi, N. Krishnan, et al, "On the impact of oscillator phase noise on the uplink performance in a massive MIMO-OFDM system," [arxiv.org/abs/1405.0669](https://arxiv.org/abs/1405.0669).
8. O. H. Salim, W. Xiang, A. A. Nasir, G. Wang, and H. Mehrpouyan, "Joint data detection and phase noise mitigation for light field video transmission in MIMO-OFDM systems," [arxiv.org/abs/1602.02834](https://arxiv.org/abs/1602.02834)
9. S. Wu and Y. Bar-Ness, "Multiple phase noise correction for OFDM/SDMA," in *Proc. IEEE Globle Telecommun. Conf. (GLOBECOM)*, Dec. 2003.
10. A. Puglielli, G. LaCaille, A. M. Niknejad, et al., "Phase noise scaling and tracking in OFDM multi-user beamforming arrays," in *Proc. IEEE Int. Commun. Conf. (ICC)*, May 2016.
11. A. Pitarkoilis, E. Björnson, Erik G. Larsson, "Performance of the massive MIMO uplink with OFDM and phase noise," *IEEE Commun. Lett.* **20**, 8, pp. 1595-1598, Aug. 2016.
12. X. Chen, "OFDM based multi-node transmission in the presence of phase noises for small cell backhaul," *IEEE Commun. Lett.*, vol. 21, no. 5, pp. 1207-1210, May 2017.
13. P. Graczyk, G. Letac, and H. Massam, "The complex Wishart distribution and the symmetric group," *Annals of Statistics*, **31**, 1, pp. 287-309, 2003.
14. R. He, Q. Li, Bo Ai, et al., "A Kernel-power-density based algorithm for channel multipath components clustering," *IEEE Trans. Wireless Commun.*, vol. 16, no. 11, pp. 7138 - 7151 , Nov. 2017.
15. K. Guan, B. Ai, A. Fricke, et al., "Excess propagation loss of semi-closed obstacles for inter/intra-device communications in the millimeter-wave range," *Journal of Infrared, Millimeter, and Terahertz Waves*, vol. 37, no. 7, pp. 676-690, July 2016.